

# Detecting $\pi$ -phase superfluids with $p$ -wave symmetry in a quasi-1D optical lattice

Bo Liu,<sup>1,2</sup> Xiaopeng Li,<sup>3</sup> Randall G. Hulet,<sup>4</sup> and W. Vincent Liu<sup>1,2</sup>

<sup>1</sup>Department of Physics and Astronomy, University of Pittsburgh, Pittsburgh, PA 15260, USA

<sup>2</sup>Wilczek Quantum Center, Zhejiang University of Technology, Hangzhou 310023, China

<sup>3</sup>Condensed Matter Theory Center and Joint Quantum Institute,  
University of Maryland, College Park, MD 20742, USA

<sup>4</sup>Department of Physics and Astronomy and Rice Quantum Institute, Rice University, Houston, TX 77005, USA

We propose an experimental protocol to study  $p$ -wave superfluidity in a spin-polarized cold Fermi gas tuned by an  $s$ -wave Feshbach resonance. A crucial ingredient is to add a quasi-1D optical lattice and tune the fillings of two spins to the  $s$  and  $p$  band, respectively. The pairing order parameter is confirmed to inherit  $p$ -wave symmetry in its center-of-mass motion. We find that it can further develop into a state of unexpected  $\pi$ -phase modulation in a broad parameter regime. Measurable quantities are calculated, including time-of-flight distributions, radio-frequency spectra, and *in situ* phase-contrast imaging in an external trap. The  $\pi$ -phase  $p$ -wave superfluid is reminiscent of the  $\pi$ -state in superconductor-ferromagnet heterostructures but differs in symmetry and origin. If observed, it would represent another example of  $p$ -wave pairing, first discovered in He-3 liquids.

Coexistence of singlet  $s$ -wave superconductivity with ferromagnetism is a long-standing issue in condensed matter physics [1]. One of the most interesting phenomena is the so-called  $\pi$ -phase achieved in artificially fabricated heterostructures of ferromagnetic and superconducting layers [2–5], where the relative phase of the superconducting order parameter between neighboring superconducting layers is  $\pi$ . The  $\pi$ -state offers new ways for studying the interplay between superconductivity and magnetism and has potential application for quantum computing in building up superconducting qubits through the  $\pi$  phase shift [6, 7]. Different settings for its realization have been discussed, such as in high  $T_c$  superconductors [8–10] and in spin-dependent optical lattices [11].

In this letter, first we show that an unconventional  $p$ -wave  $\pi$ -phase superfluid state emerges in the experimental system of a Fermi gas in a quasi-one dimensional optical lattice [12]. Then we propose experimental protocols for observing this novel state by tuning the spin polarization. This is reminiscent of the  $\pi$ -state in superconductor-ferromagnet heterostructures [1]. However, the  $\pi$  phase shift of the superfluid gap here arises from a different mechanism—the relative inversion of the single particle band structures ( $s$ - and  $p$ -orbital bands) of the two spin components involved in the pairing. As a result of this novel pairing mechanism, such a  $\pi$ -phase superfluid state has a distinctive feature—a center-of-mass (COM)  $p$ -wave symmetry, which distinguishes it from other  $\pi$ -states in previous studies [1, 11]. We map out the phase diagram as a function of controllable experimental parameters—atom density and spin polarization. There is a large window for the predicted COM  $p$ -wave  $\pi$ -phase superfluids in the phase diagram at low density and it occurs at higher critical temperature in relative scales, enhancing its potential for experimental realization. Striking signatures are calculated for experimental detection: (1) the shape of the density distribution in time-of-flight shows dramatic changes resulting from the pairing between different parity orbitals (i.e.,  $s$  and  $p$  orbitals); (2) distinctive features are found in the density of states (DOS) such as the existence of the finite gap and midgap peak, which can be detected via radio frequency (rf) spectroscopy; (3) in

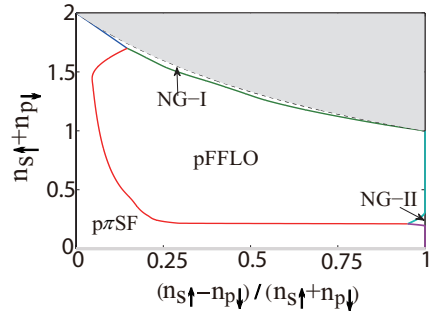


FIG. 1: Zero temperature phase diagram as a function of lattice filling and polarization when  $t_p/t_s = 8$ ,  $t'_p/t_s = 0.05$ ,  $t'_s/t_s = 0.05$  and  $U/t_s = -9$ .  $p\pi$ SF and  $p$ FFLO stand for different modulated COM  $p$ -wave superfluid states with the center-of-mass momentum of Cooper pairs located at  $\mathbf{Q} = (\pi/a, 0, 0)$  and  $\mathbf{Q} \neq (\pi/a, 0, 0)$ , respectively. NG-I refers to a normal gas (without pairing) where the  $|s \uparrow\rangle$  band is fully filled while the  $|p \downarrow\rangle$  band is partially filled. NG-II is another kind of normal state where the  $|s \uparrow\rangle$  band is partially filled while the  $|p \downarrow\rangle$  band is nearly empty. The grey area is forbidden due to the Fermi statistics constraint on the lattice filling. The grey line stands for the empty state.

the presence of a shallow trap background, the density (including atom number density and pair density) distributions in real space exhibit shell structures composed of the predicted  $p$ -wave superfluids. The orbital degrees of freedom play an essential role here; recently the research of higher orbital bands in optical lattices has evolved rapidly [13]. For  $p$ -band fermions with attractive interaction, the chiral center-of-mass  $p$ -wave superfluidity in 2D [14] and superfluids similar to the Fulde-Ferrell-Larkin-Ovchinnikov [15] were found in theoretical studies. As we shall show with the model below, the pairing composed of different parity orbital fermions will lead to unexpected COM  $p$ -wave  $\pi$ -phase superfluids.

*Effective model.* Consider a Fermi gas with  $s$ -wave attraction composed of two hyperfine states, to be referred to as spin  $\uparrow$  and  $\downarrow$ , loaded in a strongly anisotropic 3D cu-

bic optical lattice. In particular, we consider the lattice potential  $V_{OL} = \sum_{\alpha=x,y,z} V_{\alpha} \sin^2(k_L \mathbf{r}_{\alpha})$  with lattice strengths  $V_z = V_y \gg V_x$ , where  $k_L$  is the wavevector of the laser fields. In the deep lattice limit, the lattice potential at each site can be approximated by a harmonic oscillator and the lowest two energy levels are  $s$  and  $p_x$  orbital states for the lattice potential considered here, while other levels such as  $p_y$  and  $p_z$  orbitals are well separated in energy. In the following, the  $p_x$  orbital state is simply called the  $p$  orbital. Due to the strong confinement of the lattice potential in  $y$  and  $z$  directions, the system is dynamically separated into an array of quasi-one dimensional tubes. Further, let the gas be tuned with spin imbalance by the techniques developed in recent experiments [16–18]. A key condition proposed here is to tune the imbalance sufficiently that the spin  $\uparrow$  and  $\downarrow$  Fermi levels reside in the  $s$  and  $p$  orbital bands respectively in order to hybridize the spin and orbital degrees of freedom. In the tight binding regime, the system is described by a multi-orbital Fermi Hubbard model

$$\begin{aligned}
H = & -t_s \sum_{\mathbf{r}} C_{s\uparrow}^{\dagger}(\mathbf{r}) C_{s\uparrow}(\mathbf{r} + \vec{e}_x) + t_p \sum_{\mathbf{r}} C_{p\downarrow}^{\dagger}(\mathbf{r}) C_{p\downarrow}(\mathbf{r} + \vec{e}_x) \\
& - t'_s \sum_{\mathbf{r}} [C_{s\uparrow}^{\dagger}(\mathbf{r}) C_{s\uparrow}(\mathbf{r} + \vec{e}_y) + C_{s\uparrow}^{\dagger}(\mathbf{r}) C_{s\uparrow}(\mathbf{r} + \vec{e}_z)] \\
& - t'_p \sum_{\mathbf{r}} [C_{p\downarrow}^{\dagger}(\mathbf{r}) C_{p\downarrow}(\mathbf{r} + \vec{e}_y) + C_{p\downarrow}^{\dagger}(\mathbf{r}) C_{p\downarrow}(\mathbf{r} + \vec{e}_z)] + h.c. \\
& - \mu_{\uparrow} \sum_{\mathbf{r}} C_{s\uparrow}^{\dagger}(\mathbf{r}) C_{s\uparrow}(\mathbf{r}) - \mu_{\downarrow} \sum_{\mathbf{r}} C_{p\downarrow}^{\dagger}(\mathbf{r}) C_{p\downarrow}(\mathbf{r}) \\
& + U \sum_{\mathbf{r}} C_{s\uparrow}^{\dagger}(\mathbf{r}) C_{s\uparrow}(\mathbf{r}) C_{p\downarrow}^{\dagger}(\mathbf{r}) C_{p\downarrow}(\mathbf{r}), \tag{1}
\end{aligned}$$

where  $t_s$  and  $t_p$  are the hopping amplitudes along the  $x$  direction for the  $s$  and  $p$  band fermions, respectively, while  $t'_s$  and  $t'_p$  are the hopping amplitude along the  $y$  and  $z$  directions. All the hopping amplitudes as introduced in Eq. (1) are positive and the relative signs before them are fixed by the parity symmetry of the  $s$  and  $p$  orbital wave functions.  $C_{\nu\sigma}(\mathbf{r})$  is a fermionic annihilation operator for the spin  $\sigma$  component ( $\uparrow$  and  $\downarrow$ ) fermion with the localized  $\nu$  ( $s$  and  $p$ ) orbital located at the lattice site  $\mathbf{r}$ , and  $\mu_{\sigma}$  is the corresponding chemical potential. The onsite interaction (last term in Eq. (1)) is of the density-density type and arises from the interaction between two hyperfine states, which is highly tunable through the  $s$ -wave Feshbach resonance in the ultracold atomic gases. Here we assume that the interaction strength is much smaller than the band gap. Therefore, the  $s$ -band fully filled spin down fermions are dynamically inert which are not included in the Hamiltonian (Eq. (1)). In this work, we focus on the case with attractive interaction where superfluidity is energetically favorable.

*Phase diagram at zero temperature.* In order to study the superfluidity in our system, we apply the mean-field approximation and assume the superfluid pairing is between different parity orbitals, i.e., between  $|s \uparrow\rangle$  and  $|p \downarrow\rangle$  states, in a general form  $\Delta(\mathbf{r}) = U \langle C_{p\downarrow}(\mathbf{r}) C_{s\uparrow}(\mathbf{r}) \rangle = \sum_{m=1}^M \Delta_m \exp(i\mathbf{Q}_m \cdot \mathbf{r})$ ,

where  $M$  is an integer. Then, the Hamiltonian in the momentum space reads

$$\begin{aligned}
H_{MF} = & \sum_{\mathbf{k}} \varepsilon_s(\mathbf{k}) C_{s\uparrow}^{\dagger}(\mathbf{k}) C_{s\uparrow}(\mathbf{k}) + \sum_{\mathbf{k}} \varepsilon_p(\mathbf{k}) C_{p\downarrow}^{\dagger}(\mathbf{k}) C_{p\downarrow}(\mathbf{k}) \\
& + \sum_{m=1}^M \sum_{\mathbf{k}} (\Delta_m^* C_{p\downarrow}(-\mathbf{k} + \mathbf{Q}_m) C_{s\uparrow}(\mathbf{k}) + h.c.) \\
& - N \sum_{m=1}^M \frac{|\Delta_m|^2}{U}, \tag{2}
\end{aligned}$$

where  $\varepsilon_s(\mathbf{k}) = -2t_s \cos k_x a - 2t'_s (\cos k_y a + \cos k_z a) - \mu_{\uparrow}$ ,  $\varepsilon_p(\mathbf{k}) = 2t_p \cos k_x a - 2t'_p (\cos k_y a + \cos k_z a) - \mu_{\downarrow}$ ,  $\mathbf{k}$  is the lattice momentum in the first Brillouin zone (BZ),  $N$  is the total number of lattice sites and  $a$  is the lattice constant.

A fully self-consistent mean field calculation for the space-dependent order parameter is numerically challenging. We restrict our discussion to two forms of a variational ansatz. The first one is analogous to the Fulde-Ferrell state, where it assumes that  $M = 1$  and the order parameter reads  $\Delta(\mathbf{r}) = \Delta \exp(i\mathbf{Q} \cdot \mathbf{r})$ . The absolute value of superfluid gap is a constant, but the phase alternates from site to site. The second one is chosen by  $M = 2$ ,  $\Delta_1 = \Delta_2 = \frac{\Delta}{2}$  and  $\mathbf{Q}_1 = -\mathbf{Q}_2$ , namely  $\Delta(\mathbf{r}) = \Delta \cos(\mathbf{Q} \cdot \mathbf{r})$ , which is an analogue of the Larkin-Ovchinnikov state. This variational approach adopted here was previously justified by density-matrix-renormalization-group methods [19]. Here we choose  $\mathbf{Q}$  pointing along the  $x$  direction, say  $\mathbf{Q} = Q(1, 0, 0)$  to fully gap the Fermi surface of this quasi-one dimensional system. For FF like states, the mean-field Hamiltonian in Eq. (2) can be diagonalized through the Bogoliubov transformation. The grand canonical potential of the system reads

$$\Omega = \sum_{\mathbf{k}} \left[ \sum_{\gamma=\pm} -\frac{1}{\beta} \ln(1 + \exp(-\beta \zeta_{\gamma}(\mathbf{k}))) + \varepsilon_p(\mathbf{k}) \right] - N \frac{|\Delta|^2}{U}, \tag{3}$$

where  $\zeta_{\pm}(\mathbf{k}) = \frac{1}{2} [\varepsilon_s(\mathbf{k}) - \varepsilon_p(-\mathbf{k} + \mathbf{Q}) \pm \sqrt{[\varepsilon_s(\mathbf{k}) + \varepsilon_p(-\mathbf{k} + \mathbf{Q})]^2 + 4|\Delta|^2}]$  is the quasi-particle dispersion. While for the case of LO-like states, the Hamiltonian can not be diagonalized analytically. However, the pairing terms link the one-particle states with momenta lying a single line in the BZ. Therefore, we can solve the resulting eigenproblem numerically for relatively large systems.

From our numerics, we find that the free energy of the analogous LO states is always lower than that of the FF like phases, except at  $\mathbf{Q} = (\pi/a, 0, 0)$ , where the FF and LO-like ansatz are equivalent. So the ground state of the system is a COM  $p$ -wave superfluid state with modulated pairing order parameter  $\propto \cos(\mathbf{Q} \cdot \mathbf{r})$ , which breaks the translational symmetry spontaneously. Qualitatively, that is because the  $\pm\mathbf{Q}$  pairing opens gaps on both sides of the Fermi surface, taking advantage of the available phase space for pairing, while the FF states only open a gap on one side. Since the dispersion of the  $p$  band is inverted with respect to that of the  $s$  band,

the pairing occurs between fermions with center-of-mass momentum  $Q \simeq k_{F\uparrow} + k_{F\downarrow}$ , where  $k_{F\uparrow}$  and  $k_{F\downarrow}$  are the two relevant Fermi momenta. When the occupation numbers of  $|s \uparrow\rangle$  and  $|p \downarrow\rangle$  states are equal, the  $\pi$ -phase superfluid state with  $\mathbf{Q} = (\pi/a, 0, 0)$  is the ground state of the system. In real space, the pairing order parameter is a function of staggered signs along the  $x$  direction and obeys  $\Delta(\mathbf{r}) = -\Delta(\mathbf{r} + a\mathbf{e}_x)$  when combined with the periodicity  $\Delta(\mathbf{r}) = \Delta(\mathbf{r} + 2a\mathbf{e}_x)$ . The  $\pi$  phase shift of the superfluid gap here arises from the relatively inverted single particle band structures directly, unlike in the conventional FFLO state [20]. The predicted  $\pi$ -phase superfluid state is found to be quite robust. Even when the occupation number difference between  $|s \uparrow\rangle$  and  $|p \downarrow\rangle$  states is finite, the  $\pi$ -phase superfluid state is still the ground state. Particularly in the low density region  $n_s + n_p \ll 1$ , there is a large window for this  $\pi$ -state.

When the polarization  $p = \frac{n_{s\uparrow} - n_{p\downarrow}}{n_{s\uparrow} + n_{p\downarrow}}$  is sufficiently large, the center-of-mass momentum will become incommensurate with the underlying lattice and this incommensurate COM  $p$ -wave state will be referred to as pFFLO. As shown in Fig. 1, a phase diagram as a function of atom density and polarization has been obtained. When the polarization is below a critical value, the system favors the  $\pi$ -phase superfluids. Beyond this value, a first order phase transition occurs from the  $\pi$ -phase to pFFLO superfluid states. It is worth to note that a large regime of parameters is found to exist in the phase diagram, making the experimental realization of the predicted new  $p$ -wave pairing phases simpler.

Here we would like to stress two distinctions of the predicted  $p$ -wave superfluid states with different types of modulated pairing from the conventional  $s$ -band FFLO [21]. One is that the Cooper pairs here are composed of different parity orbital fermions (i.e.,  $s$  and  $p$  orbitals), which lead to the pairing order parameter with  $p$ -wave symmetry in the COM motion. The other is that the pairing order is modulated with the wavevector  $Q \simeq k_{F\uparrow} + k_{F\downarrow}$ , rather than determined by the Fermi surface mismatch.

*Experimental signatures.* The most distinctive feature of the predicted  $\pi$ -phase and pFFLO superfluids is that the pairing order parameters are spatially modulated and have  $p$ -wave symmetry in the COM motion. This leads to several characteristic experimental signatures. (A) the single particle momentum distributions exhibit unique properties in the following two aspects. The *first* one is the shape of the density distribution in time-of-flight. We calculate the spin-resolved (or equivalently orbital-resolved) density distribution in the time-of-flight measurement assuming ballistic expansion as  $\langle \tilde{n}_{\nu\sigma}(x) \rangle_t = \left(\frac{m}{\hbar t}\right)^2 \sum_{\tilde{k}_y, \tilde{k}_z} \phi_\nu^*(\tilde{\mathbf{k}}) \phi_\nu(\tilde{\mathbf{k}}) \langle C_{\nu\sigma}^\dagger(\mathbf{k}) C_{\nu\sigma}(\mathbf{k}) \rangle$ , where  $\tilde{\mathbf{k}} = m\mathbf{r}/(\hbar t)$ ,  $\phi_\nu(\tilde{\mathbf{k}})$  is the Fourier transform of the  $\nu$ -orbital band Wannier function  $\phi_\nu(\mathbf{r})$  and  $\mathbf{k} = \tilde{\mathbf{k}} \bmod \mathbf{G}$  is the momentum in the first BZ corresponding to  $\tilde{\mathbf{k}}$  ( $\mathbf{G}$  is the primitive reciprocal lattice vector). As shown in Fig. 2, the highest peak for  $p$  band fermions is shifted from zero momentum resulting from the non-trivial profile of the  $p$ -wave Wannier function superposed on the density distributions, dis-

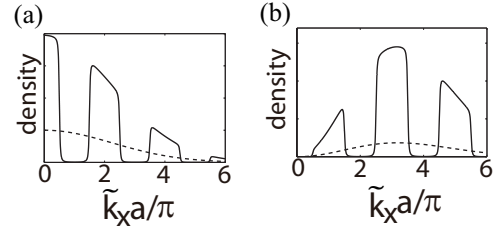


FIG. 2: Prediction of spin-resolved density distribution in time-of-flight, in (a) for  $|s \uparrow\rangle$  fermions, while in (b) for  $|p \downarrow\rangle$  fermions. The solid line shows the density defined in the main text along the  $\tilde{k}_x$ -axis. The dash lines show the intensities of the Wannier orbital functions  $\propto |\phi_\nu(\tilde{k}_x)|^2$  for comparison. Other parameters are  $n_{s\uparrow} = 0.5$ ,  $n_{p\downarrow} = 0.5$ ,  $t_p/t_s = 8$ ,  $t'_p/t_s = 0.05$ ,  $t'_s/t_s = 0.05$  and  $U/t_s = -9$ .

tinguished from the  $s$  orbital fermions. The *second* aspect is a mirror-translational symmetry of the axial density distributions of  $|s \uparrow\rangle$  and  $|p \downarrow\rangle$  fermions for the  $\pi$ -phase superfluid state. Following the standard analysis [12, 22], we define the axial density distribution in the momentum space as  $n_{\nu\sigma}^a(k_x) = \frac{1}{(2\pi)^2} \int dk_y dk_z \langle C_{\nu\sigma}^\dagger(\mathbf{k}) C_{\nu\sigma}(\mathbf{k}) \rangle$  for  $|s \uparrow\rangle$  and  $|p \downarrow\rangle$  fermions, respectively. From Eq. (3), the atom density distributions of  $|s \uparrow\rangle$  and  $|p \downarrow\rangle$  fermions can be calculated through  $n_{\nu\sigma}(\mathbf{k}) = \frac{\partial \Omega}{\partial \mu_\sigma}$ . In the zero temperature, we find that  $n_{s\uparrow}(\mathbf{k}) = n_{p\downarrow}(\mathbf{Q} - \mathbf{k}) = \frac{-[\varepsilon_s(\mathbf{k}) + \varepsilon_p(-\mathbf{k} + \mathbf{Q})] + \sqrt{\mathbb{E}(\mathbf{k})}}{2\sqrt{\mathbb{E}(\mathbf{k})}}$  where  $\mathbb{E}(\mathbf{k}) = [\varepsilon_s(\mathbf{k}) + \varepsilon_p(-\mathbf{k} + \mathbf{Q})]^2 + 4|\Delta|^2$  and  $\mathbf{Q} = (\pi/a, 0, 0)$ . Therefore, the axial density distributions defined above satisfy the relation  $n_{s\uparrow}^a(k_x) = n_{p\downarrow}^a(\pi/a - k_x)$ . It is also confirmed in our numerics as shown in Fig. 3(c). These signatures can be detected through polarization phase contrast imaging [12].

(B) the COM  $p$ -wave superfluid state here has the spatially nonuniform pairing order parameter, making it different from conventional  $p$ -wave superfluids. This leads to crucial difference in Bogoliubov quasi-particle spectra. A finite energy gap is shown in the spin-resolved (or equivalently the orbital-resolved) density of states (DOS) for the  $\pi$ -phase superfluids (Fig. 3a). Such spin-resolved DOS is calculated as  $\rho_{\nu\sigma}(E) = \frac{1}{2} \sum_n [ |u_n^{\nu\sigma}|^2 \delta(E - \zeta_n) + |v_n^{\nu\sigma}|^2 \delta(E + \zeta_n) ]$ , where  $(u_n^{\nu\sigma}, v_n^{\nu\sigma})^T$  is the eigenvector corresponding to the eigenenergy  $\zeta_n$  of the mean-field Hamiltonian Eq. (2) and the summation runs over all the eigenenergy. This finite gap in the DOS gives direct evidence of superfluidity. For the pFFLO state, there is a midgap peak in the DOS, shown in Fig. 3(b). This midgap peak results from the spatially modulated pairing order parameter which signifies the emergence of Andreev bound states [23]. The energy gap and midgap peak are found in the spin-resolved DOS for both  $|s \uparrow\rangle$  and  $|p \downarrow\rangle$  fermions. For example, the DOS of  $|s \uparrow\rangle$  fermions is shown in Fig. 3. Such spin-resolved DOS signatures can be detected via radio frequency (rf) spectroscopy [24–26], giving an experimental plausible probe of the predicted  $p$ -wave superfluids.

(C) the predicted COM  $p$ -wave superfluids require neither spin-orbital coupling nor an induced second order effective

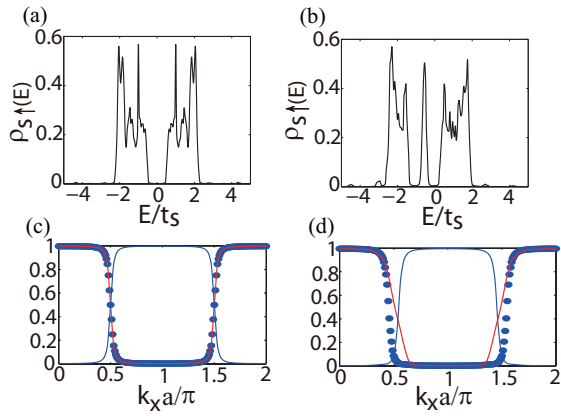


FIG. 3: Top row plots density of states (DOS)  $\rho_{s\uparrow}(E)$ , (a) showing the finite energy gap for the  $\pi$ -phase superfluid state and (b) showing the midgap peak for pFFLO resulting from Andreev bound states. Bottom row plots the axial density distributions of  $|s \uparrow\rangle$  and  $|p \downarrow\rangle$  fermions in momentum space for each of  $\pi$ -phase (c) and pFFLO (d). The red and blue solid lines show  $n_{s\uparrow}^a(k_x)$  and  $n_{p\downarrow}^a(k_x)$  respectively, while the blue dots show  $n_{p\downarrow}^a(Q - k_x)$ . See main text for the definition of  $\rho_{s\uparrow}(E)$  and  $n_{\nu\sigma}^a(\mathbf{k})$ . For the pFFLO state in (b), since there is a large polarization which can be considered as an effective external magnetic field, it leads to a shift of the density of states. Therefore, the midgap peak in (b) is not at  $E = 0$ . In (a) and (c), we choose  $n_{s\uparrow} = 0.5$  and  $n_{p\downarrow} = 0.5$ , while in (b) and (d),  $n_{s\uparrow} = 0.52$  and  $n_{p\downarrow} = 0.45$ . Other parameters are the same as in Fig. 1.

$p$ -wave interaction. It arises directly from a purely  $s$ -wave two-body attraction. This leads to a significantly improved transition temperature, which is confirmed by our direct calculation of finite temperature phase transitions for the model Hamiltonian in Eq. (1)—see Fig. 4 for the phase diagram. The transition temperature of the predicted COM  $p$ -wave superfluids is indeed significantly improved as compared to other conventional relative  $p$ -wave superfluids [27, 28]. For instance, suppose a quasi-1D optical lattice has the lattice depth  $V_x = 5E_r$ ,  $V_y = V_z = 18E_r$  and the wavelength of the lattice beams is 1064nm, the mean-field superfluid transition temperature can reach around 60nK when the  $s$ -wave scattering length between  ${}^6\text{Li}$  atoms is  $a_s \simeq 326a_0$  [29], where  $a_0$  denotes the Bohr radius. Further increasing  $a_s$ , to around  $600a_0$ , the transition temperature can reach around  $0.2\mu\text{K}$ , or even higher.

*Shell structure in a trap.* In the following, we will discuss the effect of a harmonic trapping potential superposed on the optical lattices. Assuming that the harmonic trapping potential is sufficiently shallow compared with the lattice depth, it is natural to apply the local density approximation (LDA) and let the chemical potential vary as a function of the position. Here we consider the trapping potential in the  $x$  direction. Fig. 5 shows various shell structures by our calculation. When the polarization is small, the region in the center of trap is the  $\pi$ -phase superfluid, surrounded by a normal gas shell. While increasing the polarization, the region in the center of trap is no longer a superfluid, but a normal gas, surrounded by a pF-

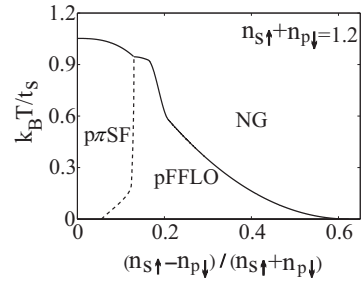


FIG. 4: Finite temperature phase diagram as a function of temperature and polarization at a certain lattice filling when  $t_p/t_s = 8$ ,  $t'_p/t_s = 0.05$ ,  $t'_s/t_s = 0.05$  and  $U/t_s = -9$ .

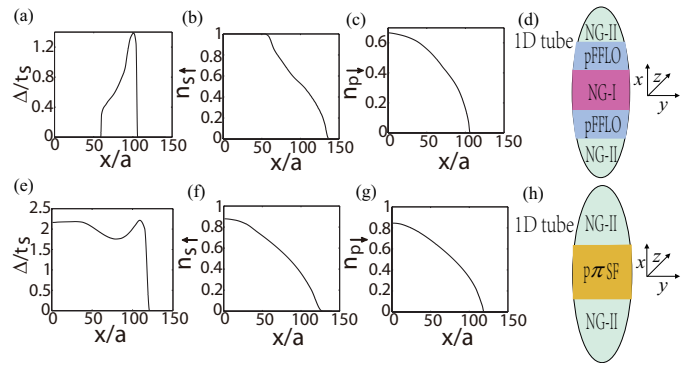


FIG. 5: Shell structures with a background trapping potential. The superfluid gap  $\Delta$  and density profile  $n_{s\uparrow}$  and  $n_{p\downarrow}$  of  $|s \uparrow\rangle$  and  $|p \downarrow\rangle$  fermions are shown as a function of the coordinate  $x$ , when  $t_p/t_s = 8$ ,  $t'_p/t_s = 0.05$ ,  $t'_s/t_s = 0.05$  and  $U/t_s = -9$ . The polarization  $P = \frac{N_{s\uparrow} - N_{p\downarrow}}{N_{s\uparrow} + N_{p\downarrow}}$  is fixed at 0.3 and 0.03 for the first and second row, respectively. The frequency of the harmonic trap is chosen to be 120 Hz.

FLO superfluid shell, which in turn is surrounded by another shell of a normal gas. The density profile of  $|s \uparrow\rangle$  and  $|p \downarrow\rangle$  fermions along the  $x$  direction are also demonstrated in Fig. 5, which can be detected through *in situ* phase-contrast imaging, providing an experimental plausible probe in a trapped atomic Fermi gas [12].

Let us take a specific experimental system,  ${}^6\text{Li}$  atoms, as an example. This Fermi gas is typically prepared with a total atom number around  $10^5$  in a trap [12, 16]. In the recent experiment, it is loaded in an optical lattice and cooled down to the antiferromagnetic (Néel) transition scale [29]. At the center of the trap, the density of one particle per site is maintained. One can take advantage of this experimental development to achieve the  $\pi$ -phase  $p$ -wave state. One apparent method is to have a higher density, say, through tightening of the trap potential or filling more atoms into the lattice initially [30–32]. Taking the peak density of atoms to be around  $2 \times 10^{13} \text{cm}^{-3}$ , the central filling of the lattice system is three particles per site when the lattice constant  $a = 532\text{nm}$ . Another method is through tuning the polarization parameter of

the two hyperfine-spin components, so to populate one and only one of the two components of atoms into the  $p$ -orbital band. The two methods may be combined to optimize the experiment.

*Conclusion.* We propose that the pairing between different parity orbital fermions can lead to a  $p$ -wave  $\pi$ -phase superfluid state. The origin of the  $\pi$  phase shift of the pairing order is distinct from the previous studies of  $\pi$ -states. We show that the predicted  $\pi$ -phase here occurs in a broad range in the phase diagram especially in the low density region. Increasing polarization, we find a phase transition from the  $\pi$ -phase state to an incommensurate COM  $p$ -wave superfluid. Signatures of the predicted  $p$ -wave superfluid states are calculated for time-of-flight and spectroscopic measurements in the regime of atom density and spin polarization deemed experimentally accessible. The transition temperature and various shell structures with a background trapping potential are obtained for future experiments to explore these new forms of  $p$ -wave superfluid states.

*Acknowledgements.* This work is supported by AFOSR (FA9550-12-1-0079), ARO (W911NF-11-1-0230), Overseas Collaboration Program of NSF of China No. 11429402 sponsored by Peking University, the Charles E. Kaufman Foundation, and The Pittsburgh Foundation (B. L. and W. V. L.). X. L. is supported by LPS-MPO-CMTC, JQI-NSF-PFC and ARO-Atomtronics-MURI. R. G. H. acknowledges support from ARO Grant No. W911NF-13-1-0018 with funds from the DARPA OLE program, NSF, ONR, the Welch Foundation (Grant No. C-1133), and ARO-MURI Grant No. W911NF-14-1-0003.

- 
- [1] A. I. Buzdin, *Rev. Mod. Phys.* **77**, 935 (2005).  
 [2] V. V. Ryazanov, V. A. Oboznov, A. Y. Rusanov, A. V. Veretennikov, A. A. Golubov, and J. Aarts, *Phys. Rev. Lett.* **86**, 2427 (2001).  
 [3] T. Kontos, M. Aprili, J. Lesueur, F. Genêt, B. Stephanidis, and R. Boursier, *Phys. Rev. Lett.* **89**, 137007 (2002).  
 [4] H. Sellier, C. Baraduc, F. m. c. Lefloch, and R. Calemczuk, *Phys. Rev. B* **68**, 054531 (2003).  
 [5] V. A. Oboznov, V. V. Bol'ginov, A. K. Feofanov, V. V. Ryazanov, and A. I. Buzdin, *Phys. Rev. Lett.* **96**, 197003 (2006).  
 [6] J. E. Mooij, T. P. Orlando, L. Levitov, L. Tian, C. H. van der Wal, and S. Lloyd, *Science* **285**, 1036 (1999).  
 [7] L. B. Ioffe, V. B. Geshkenbein, M. V. Feigel'man, A. L. Fauchere, and G. Blatter, *Nature* **398**, 679 (1999).  
 [8] C. Bernhard, J. L. Tallon, C. Niedermayer, T. Blasius, A. Golnik, E. Brücher, R. K. Kremer, D. R. Noakes, C. E. Stronach, and E. J. Ansaldo, *Phys. Rev. B* **59**, 14099 (1999).  
 [9] A. C. McLaughlin, W. Zhou, J. P. Attfield, A. N. Fitch, and J. L. Tallon, *Phys. Rev. B* **60**, 7512 (1999).  
 [10] O. Chmaissem, J. D. Jorgensen, H. Shaked, P. Dollar, and J. L. Tallon, *Phys. Rev. B* **61**, 6401 (2000).  
 [11] I. Zapata, B. Wunsch, N. T. Zinner, and E. Demler, *Phys. Rev. Lett.* **105**, 095301 (2010).  
 [12] Y.-a. Liao, A. S. C. Rittner, T. Paprotta, W. Li, G. B. Partridge, R. G. Hulet, S. K. Baur, and E. J. Mueller, *Nature* **467**, 567 (2010).  
 [13] For a perspective and brief review, see, for example, M. Lewenstein and W. V. Liu, *Optical lattices: Orbital dance. Nat Phys* **7**, 101-103 (2011).  
 [14] B. Liu, X. Li, B. Wu, and W. V. Liu, *Nat Commun* **5**, 5064 (2014).  
 [15] C. Zi, W. Yupeng, and W. Congjun, *Phys. Rev. A* **83**, 063621 (2011).  
 [16] G. B. Partridge, W. Li, R. I. Kamar, Y.-a. Liao, and R. G. Hulet, *Science* **311**, 503 (2006).  
 [17] M. W. Zwierlein, A. Schirotzek, C. H. Schunck, and W. Ketterle, *Science* **311**, 492 (2006).  
 [18] S. Nascimbène, N. Navon, K. J. Jiang, F. Chevy, and C. Salomon, *Nature* **463**, 1057 (2010).  
 [19] Z. Zhang, H.-H. Hung, C. M. Ho, E. Zhao, and W. V. Liu, *Phys. Rev. A* **82**, 033610 (2010).  
 [20] L. Radzihovsky, *Phys. Rev. A* **84**, 023611 (2011).  
 [21] G. G. Batrouni, M. H. Huntley, V. G. Rousseau, and R. T. Scalettar, *Phys. Rev. Lett.* **100**, 116405 (2008).  
 [22] T. N. De Silva and E. J. Mueller, *Phys. Rev. Lett.* **97**, 070402 (2006).  
 [23] M. R. Bakhtiari, M. J. Leskinen, and P. Törmä, *Phys. Rev. Lett.* **101**, 120404 (2008).  
 [24] S. Gupta, Z. Hadzibabic, M. W. Zwierlein, C. A. Stan, K. Dieckmann, C. H. Schunck, E. G. M. van Kempen, B. J. Verhaar, and W. Ketterle, *Science* **300**, 1723 (2003).  
 [25] C. A. Regal and D. S. Jin, *Phys. Rev. Lett.* **90**, 230404 (2003).  
 [26] Y. Shin, C. H. Schunck, A. Schirotzek, and W. Ketterle, *Phys. Rev. Lett.* **99**, 090403 (2007).  
 [27] V. Gurarie and L. Radzihovsky, *Annals of Physics* **322**, 2 (2007).  
 [28] M. Iskin and C. A. R. S. de Melo, *Phys. Rev. B* **72**, 224513 (2005).  
 [29] R. A. Hart, P. M. Duarte, T.-L. Yang, X. Liu, T. Paiva, E. Khatami, R. T. Scalettar, N. Trivedi, D. A. Huse, and R. G. Hulet, *Nature* **519**, 211 (2015).  
 [30] M. Köhl, H. Moritz, T. Stöferle, K. Günter, and T. Esslinger, *Phys. Rev. Lett.* **94**, 080403 (2005).  
 [31] U. Schneider, L. Hackermüller, S. Will, T. Best, I. Bloch, T. A. Costi, R. W. Helmes, D. Rasch, and A. Rosch, *Science* **322**, 1520 (2008).  
 [32] R. Jordens, N. Strohmaier, K. Gunter, H. Moritz, and T. Esslinger, *Nature* **455**, 204 (2008).